

Structural Change of Cooper Pairs and Momentum-dependent Gap in Color Superconductivity

Hiroaki Abuki and Tetsuo Hatsuda^y

Department of Physics, University of Tokyo, Tokyo 113-0033, Japan

Kazunori Itakura^z

RIKEN BNL Research Center, Brookhaven National Laboratory, Upton, NY 11973, USA

(February 8, 2020)

The two-flavor color superconductivity is studied with a special attention to the spatial momentum dependence of the gap and to the spatial structure of Cooper pairs. The gap at extremely high baryon density ($\sim 10^{10} \rho_0$ with ρ_0 being the normal nuclear matter density) is shown to have a sharp peak near the Fermi surface due to the weak-coupling nature of QCD. On the other hand, the gap is a smooth function of the momentum at lower densities ($\sim 10 \rho_0$) due to strong color magnetic and electric interactions. To study the structural change of Cooper pairs from high density to low density, quark correlations in the color superconductor are studied in the momentum space and in the coordinate space. The size of the Cooper pair is shown to become comparable to the averaged inter-quark distance at low densities. Also, effects of the momentum-dependent quark-gluon vertex and the coupling to the antiquark pairing, which are both small at high density, are shown to be non-negligible at low densities. These features are highly contrasted to the standard BCS superconductivity in metals.

I. INTRODUCTION

Because of the asymptotic freedom and the Debye screening in QCD, the deconfined quark matter is expected to be realized for baryon densities much larger than the normal nuclear matter density [1]. Furthermore, any attractive quark-quark interaction in the cold quark matter causes an instability of the Fermi surface by the formation of Cooper pairs and leads to the color superconducting phase [2,6].

For extremely high baryon density in which the gluonic interaction is weak, the formation of Cooper pairs takes place only in a small region near the Fermi surface. In this weak-coupling regime, there are numerous studies of the superconducting gap at and near the Fermi surface. In particular, the effect of dynamical screening of the long-range color-magnetic interaction (the Landau damping) has been investigated extensively [7,12].

On the other hand, for relatively low baryon densities, the gluonic attraction becomes effective for all quarks inside the Fermi sea and sizable Cooper pairing takes place for wide range of momentum away from the Fermi surface. This is not only because the QCD coupling is not small at low densities but also because the gluonic interaction does not suffer from the ultraviolet cut-off, which is in contrast to the phonon interaction with an intrinsic Debye cut-off in the BCS-type superconductivity [13]. Therefore, the quark matter at relatively low densities may have properties qualitatively different from the BCS-type superconductor. In particular, spatial momentum dependence of the gap, usefulness of the Fermi surface, quark-quark correlations in the superconductor and the spatial size of Cooper pairs are the characteristic quantities which reflect the departure from the weak-coupling picture.

So far, only a few investigations have been made for the gap with spatial momentum dependence and the structure of the Cooper pairs [3,14,15]. The main purpose of this paper is to make an extensive analysis on the structural change of the color superconductor from high to low densities.

Throughout the paper, we limit our discussions to 2-flavor color superconductivity partly because our primary interests are in low densities and partly because the analysis is simpler than in the three-flavor case [16]. To investigate how the weak-coupling picture is modified at low densities in a qualitative manner, we adopt a model of static one-gluon exchange with a minimal dynamical correction from the Landau damping. Although we adopt a specific model for the gluon exchange, similar analysis can be equally carried out for other nonlocal effective interactions used in the literatures [17,18].

abuki@nt.phys.s.u-tokyo.ac.jp

^yhatsuda@phys.s.u-tokyo.ac.jp

^zitakura@bnl.gov

This paper is organized as follows. In Sect. II, we define our model and derive relevant gap equations. We first consider the weak-coupling region at high density and discuss the general properties of the gap as a function of the spatial momentum. In Sect. III, we solve the momentum-dependent gap equation numerically for a wide range of densities. A large structural change of the momentum-dependent gap will be shown. The quark and antiquark occupation numbers, the correlation of quarks in the color superconductor, and the coherence length are also investigated. Summary and concluding remarks are given in the last section. In Appendix A, the gauge dependence of the gap equation is discussed. In Appendix B, we derive the asymptotic behavior of the spatial quark-quark correlation in the weak coupling.

II. GAP EQUATION WITH SPATIAL MOMENTUM DEPENDENCE

In this section, we define our model and derive relevant gap equations in two flavor QCD with the one-gluon exchange interaction. We start with the standard Dyson-Schwinger equation for the quark self-energy with four momentum dependence [8]. Then it is reduced to a gap equation with spatial momentum dependence. General properties of the solution of our gap equation in the weak-coupling limit are also examined. The gap with spatial momentum dependence enables us to study the usefulness of the Fermi surface and the structure of Cooper pairs in the color superconductor.

Throughout this paper, we use the following notation for the four and three momenta:

$$k = (k^0; \vec{k}); \quad k = j \vec{j}; \quad \hat{k} = k = k;$$

Also, we limit ourselves to the system at zero temperature and work in the Minkowski space with the quark and gluon propagators obeying the Feynman boundary condition.

A. The model

Let us start with the definition of quark self-energy and the superconducting gap. Using the standard Nambu-Gorkov formalism with a two component Dirac spinor $\psi = (u; \bar{u})^T$, the quark self-energy $\Sigma(k)$ with the Minkowski 4-momentum k is written as

$$\Sigma(k) = S_0^{-1}(k) \quad S^{-1}(k) = \begin{pmatrix} 0 & \Sigma(k) \\ \Sigma(k) & 0 \end{pmatrix}; \quad (2.1)$$

where the superconducting gap Δ and Σ_0 enter through the off-diagonal components of Σ . The diagonal components of Σ is neglected throughout this paper [8]. $S(k)$ and $S_0(k)$ are the full and free quark propagators, respectively. The free propagator is taken to be a form $S_0^{-1}(k) = \text{diag}(\kappa^0; \kappa^1, \kappa^2, \kappa^3)^T$. We ignore the mass of u and d quarks.

To study the flavor anti-symmetric and color anti-symmetric pairing (which is the most attractive channel in the 2-flavor color superconductivity), we assume the following structure of the gap function,

$$\Delta(k) = (\gamma_2) (\text{C} \gamma_5) \hat{\Delta}(k); \quad (2.2)$$

where C is the charge conjugation, γ_2 is the Pauli matrix acting on the flavor space, γ_2 is a color anti-symmetric Gell-Mann matrix.

In the ladder approximation of the one-gluon-exchange, the Dyson-Schwinger equation for Σ is written as

$$\Sigma(k) = -i\vec{g}^2 \frac{d^4 q}{(2\pi)^4} \int_a S(q) \gamma_b D^{ab}(q - k); \quad (2.3)$$

where D^{ab} is the gluon propagator in medium and γ^a is the quark-gluon vertex which is taken to be a free one [8] for the momenta,

$$\gamma^a = \begin{pmatrix} \gamma^2 & 0 \\ 0 & (\gamma^a)^T \end{pmatrix}; \quad (2.4)$$

The gap equation is obtained from the 2-1 element of the Dyson-Schwinger (matrix) equation (2.3). The gap function $\hat{\Delta}(k)$ may be further decomposed into the quark pairing and the antiquark pairing by the positive and negative energy projection operators $\hat{P}(\hat{k}) = (1 - \hat{k}^2)^{-1/2}$:

$$\hat{\gamma}(k) = \gamma_+ (k) + \hat{\gamma}(k) + \gamma_- (k) - \hat{\gamma}(k); \quad (2.5)$$

Then the final form of the gap equation for $\gamma(k) = \gamma(k_0; k)$ reads

$$\begin{aligned} \gamma(k) = & \frac{N_c + 1}{2N_c} ig^2 \frac{d^4 q}{(2\pi)^4} \frac{1}{2} \text{tr} \left[\hat{\gamma}(k) \gamma(q) \frac{+ (q)}{q_0^2 - E_+^2(q) - j_+(q) j_-^2} \right. \\ & \left. + \frac{1}{2} \text{tr} \left[\hat{\gamma}(k) \gamma(q) \frac{(q)}{q_0^2 - E^2(q) - j_-(q) j_+^2} \right] D(q, k) \right]; \end{aligned} \quad (2.6)$$

where $E_\pm(q) (= q_\pm)$ is the reduced energy for free quarks (for + sign) and for antiquarks (for - sign).

In a general covariant gauge, the gluon propagator in the medium is written as

$$D(k) = \frac{P^T}{k^2 - \gamma_T(k)} + \frac{P^L}{k^2 - \gamma_L(k)} - \frac{k \cdot k}{k^4}; \quad (2.7)$$

where P^T, P^L are the transverse and longitudinal projectors $P_{ij}^T = \delta_{ij} \hat{k}_i \hat{k}_j$, $P_{00}^T = P_{0i}^T = 0$, and $P^L = g + k \cdot k = k^2 - P^T$. In the infrared limit $k_0 \gg j$, the longitudinal and transverse self-energies reduce to the well-known form of the Debye screening and the Landau damping [19]:

$$\gamma_L \approx m_D^2; \quad \gamma_T \approx iM^2 \frac{j_0 j}{j^2}; \quad (2.8)$$

where $m_D^2 = (N_f=2)g^2/2$ is the Debye screening mass and $M^2 = (=4)m_D^2$.

As we have mentioned in Sect. I, we will take a model of static one-gluon exchange with a minimal dynamical correction from the Landau damping. This corresponds to neglecting the k_0^2 terms in Eq. (2.7) and use the replacement Eq. (2.8). The same model is also adopted in Ref. [20].

B. Screening of collinear singularity

Since there is no Debye screening in the transverse (magnetic) part of the gluon propagator, at extremely high density, the main attraction between quarks near the Fermi surface comes from the exchange of color-magnetic gluons. This, in turn, leads to an infrared (IR) singularity by the collinear scattering of quarks, if quark momenta are restricted on the Fermi surface. In the conventional treatment of color superconductivity, such IR singularity is screened by the off-shell effect in the frequency domain, namely, dynamical screening due to the Landau damping [7].

Here we clarify how the collinear singularity is screened in our model, paying attention to the spatial momentum dependence of the gluon propagator. We discuss only the essential point in this subsection and more extensive analysis of the gap equation will be given later. Consider the real part of the magnetic gluon propagator with the on-shell quasiparticle frequency:

$$\begin{aligned} \text{Re} \frac{1}{(q - k)^2 + iM^2 j_q^+} &= \frac{(q - k)^2}{(q - k)^2 + M^4 (\frac{+}{q} \frac{+}{k})^2} \\ &= \frac{(q - k)^2 + 2qk(1 - \cos \theta)^2}{f(q - k)^2 + 2qk(1 - \cos \theta)q^3 + M^4 (\frac{+}{q} \frac{+}{k})^2}; \end{aligned} \quad (2.9)$$

where $\frac{+}{q} ((q - k)^2 + \frac{2}{+} (\frac{+}{q}; q))^{1/2}$ is the quasiparticle energy¹, and θ denotes the scattering angle between two quarks. The term $(q - k)^2$ is neglected in our model as mentioned at the end of Sect. II A. The imaginary part of the propagator is factor q^2 smaller than the real part and is also neglected here.

The propagator (2.9) appears in the gap equation together with the angular integration $\int_0^\pi d(\cos \theta)$ and the momentum integration $\int d\mathbf{q}$ as will be shown in Eq. (2.12).

If one considers the scattering of quarks only on the Fermi surface ($q = k = \mathbf{0}$), the angular integral of Eq. (2.9) reads

¹This implies that we have picked up the quasiparticle pole when we performed the frequency integral in Eq. (2.6).

$$\int_0^Z d(\cos \theta) \frac{1}{2^{-2}} \frac{1}{(1 - \cos \theta) + \frac{M^4}{(2^{-2})^2} \frac{(\frac{q}{k} + \frac{q}{k})^2}{(1 - \cos \theta)}}; \quad (2.10)$$

Because of the existence of the Landau damping proportional to M^4 , the collinear singularity from the small-angle scattering ($\theta = 0$) is screened [7].

What happens if one neglects the Landau damping ($M^2 = 0$) but takes into account the scattering above and below the Fermi surface ($q \neq k$)? In this case, the integral becomes

$$\int_0^Z d(\cos \theta) \frac{1}{2qk} \frac{1}{(1 - \cos \theta) + (q - k)^2/(2qk)}; \quad (2.11)$$

Although this integral has logarithmic singularity at $q = k$, it is integrable under $\int_0^R d\theta$. Namely, the collinear singularity in the gap equation is screened by the momentum difference $j_q^+ - k^+$ in our model of the "static" gluon propagator.²

A rough comparison of the two screening effects above can be made in terms of the variable $t (= 1 - \cos \theta)$. In the integral (2.10), the smearing from the Landau damping (LD) of the singularity takes place for $t < t_{LD}$ ($M^2 j_q^+ - k^+)^2 = 3$). On the other hand, in the integral (2.11), the smearing from the direct Fermi surface (DFS) takes place for $t < t_{DFS}$ ($(q - k)^2 = 2qk$). If one chooses a kinematical region close to the Fermi surface ($j_q^+ - k^+ \ll q - k$) with $q - k \ll 1$, one finds $t_{DFS}^2 = 2 - t_{DFS} < t_{LD}^2 = (2 - t_{DFS})^{1/3}$; for $t = e^{-\text{const}g}$ with $g \ll 1$. Therefore, the Landau damping is more important than the direct Fermi surface for quarks near the Fermi surface in our model. Away from the Fermi surface, the above estimate is not valid, and it is better to keep both effects for studying the momentum-dependent gap in the wide range of the three momentum.

C. Analytic properties of the approximate gap equation

1. Gap equation in the weak-coupling limit

Let us first study the analytic properties of the gap equation for determining the spatial momentum dependence of the gap. To obtain analytically tractable equations, we consider here the weak-coupling (high density) limit with the Landau gauge $\gamma = 0$. This "weak-coupling approximation" implies the approximation where we take only the color-magnetic interaction and the real part of γ . Contributions from the antiquarks proportional to γ and the momentum-dependent factor originating from the projection operator in Eq. (2.6) are neglected. Then, after the frequency integral by picking up quasi-particle poles in the quark propagator in Eq. (2.6), we obtain

$$+\langle k \rangle = \frac{g^2}{24^{-2}} \int_0^Z dq \frac{q^2 + (q)}{E_+^2(q) + \frac{2}{q^2}(q)} \int_0^Z d(\cos \theta) \frac{(q - k)^4}{(q - k)^6 + M^4 (\frac{q}{k} + \frac{q}{k})^2} + \frac{(q - k)^4}{(q - k)^6 + M^4 (\frac{q}{k} + \frac{q}{k})^2}; \quad (2.12)$$

where $E_+(q) = q$ and we have defined $\gamma_+(q) = \gamma_+(\frac{q}{k}; q)$ for notational simplicity. $\frac{q}{k}$ is the quasi-particle energy as a solution of $(\frac{q}{k})^2 - E_+^2(q) - \frac{2}{q^2}(\frac{q}{k}; q) = 0$.

Integration over the angular variable gives

$$+\langle k \rangle = \frac{g^2}{144^{-2}} \int_0^Z dq \frac{q^2 + (q)}{E_+^2(q) + \frac{2}{q^2}(q)} \frac{q}{k} \ln \frac{[(q + k)^6 + M^4 (\frac{q}{k} + \frac{q}{k})^2]^{\frac{1}{2}}}{(q - k)^6 + M^4 (\frac{q}{k} + \frac{q}{k})^2} + \langle \frac{q}{k} \rangle! \langle \frac{q}{k} \rangle^{\frac{1}{2}}; \quad (2.13)$$

This is the final form of an approximate gap equation in the weak-coupling limit. $\gamma_+(k)$ corresponds to the gap of the on-shell quasi-particles in the color superconductor since k_0 is taken to be $\frac{q}{k}$.

²The situation is more complex for other models of the gluon propagator such as the one with k_0^2 -terms in Eq. (2.7), which we will not discuss in this paper.

2. Gap near the Fermi surface with the Landau damping

Let us first study the effect of the Landau damping (LD) in Eq. (2.13) on the gap near the Fermi surface. For this purpose, we pick up the most singular part of the integrand by taking $q = k = \infty$ in the bracket except for the term $(\frac{q}{k})^2$ in the denominator. Then Eq. (2.13) reduces to

$${}_{+}^{\text{LD}}(k) = \frac{g^2}{72^2} \int_0^{\infty} dq \frac{\frac{1}{+}^{\text{LD}}(q)}{E_+^2(q) + j \frac{1}{+}^{\text{LD}}(q)^2} \ln \frac{(b)^2}{j \frac{1}{q}^2 + \frac{1}{k}^2}; \quad (2.14)$$

where $b = 2(2 = M)^2 = (2 = N_f)(32 = g^2)$. This equation makes sense only in the vicinity of the Fermi surface $j \ll k$ and coincides to the one derived in Ref. [11]. In the weak-coupling regime ($g = (3/2)^{1/2} \ll 1$), the approximate solution of this equation reads [11]

$${}_{+}^{\text{LD}}(k) = \frac{1}{3} \frac{g}{2} \cos \frac{j}{\frac{1}{+}^{\text{LD}}(k)} \ln \frac{j}{\frac{1}{+}^{\text{LD}}(k)} = \frac{1}{3} \frac{g}{2} \sin \frac{j}{\frac{1}{+}^{\text{LD}}(k)} \ln \frac{2b}{j} \frac{2b}{j + \frac{1}{k}}; \quad (2.15)$$

where $\frac{1}{k} = (j^2 + \frac{1}{+}^{\text{LD}}(k)^2)^{1/2}$. This solution is a symmetric function of (k) and decreases as $j \ll k$ increases. The gap at the Fermi surface is

$${}_{+}^{\text{LD}}(0) = 2b e^{-(3^2 = \frac{p}{2}) = g}; \quad (2.16)$$

Inclusion of the color-electric interaction only modifies the prefactor as $b = (2 = N_f)^{5/2} 256^{-4} = g^5$.

The characteristic form of the gap $e^{-c/g}$ in Eq. (2.16), which is not the BCS form e^{-c/g^2} , was first derived in Ref. [7]. The prefactor b was found in Refs. [8] and [11].

3. Gap without the Landau damping

Next, let us consider the case where the quark momenta are not restricted on the Fermi surface. To simplify the analysis further, we neglect the Landau damping in Eq. (2.13) and obtain

$${}_{+}^{\text{DFS}}(k) = \frac{g^2}{12^2} \int_0^{\infty} dq \frac{\frac{1}{+}^{\text{DFS}}(q)}{E_+^2(q) + j \frac{1}{+}^{\text{DFS}}(q)^2} \frac{q}{k} \ln \frac{q + k}{q - k}; \quad (2.17)$$

Since our "static" gluon propagator without the Landau damping has only a logarithmic collinear singularity $\ln j/k$, the integral over q is finite. Therefore, this gap equation still makes sense as we have mentioned in Sect. II A. To make a distinction from $\frac{1}{+}^{\text{LD}}$, we put a suffix DFS (diuse Fermi surface) to the gap in Eq. (2.17).

The integrand in the gap equation (2.17) has a similar logarithmic structure to that in Eq. (2.14). Therefore one may expect the characteristic parametric dependence of the gap $\frac{1}{+}(k) \sim b e^{-c/g}$. This is indeed the case, although the coefficient c and the prefactor b depend on the way how the collinear singularity is screened.

In a situation where k is close to the Fermi momentum and the dominant contribution in the integrand comes from the region $q \ll k$, we can make approximations such as $q \ll k \ll 1$ and $k + q \ll 2$ in Eq. (2.17). Then, we obtain

$${}_{+}^{\text{DFS}}(k) = \frac{g^2}{12^2} \int_0^{\infty} dq \frac{\frac{1}{+}^{\text{DFS}}(q)}{E_+^2(q) + j \frac{1}{+}^{\text{DFS}}(q)^2} \ln \frac{2}{E_+(q) - E_+(k)}; \quad (2.18)$$

The structure of this equation is exactly the same as that for the frequency-dependent gap with the Landau damping originally derived in Ref. [7]. This similarity is not accidental because we picked up a quark pole $q_0 = \sqrt{(q - k)^2 + p^2}$ in the frequency integral to derive the gap equation in the momentum-space (2.18), while a quark pole $q = \sqrt{p^2 + q_0^2}$ is picked up in the momentum integral to derive the gap equation in the frequency-space [7].

Using the same technique as is employed in deriving Eq. (2.15), we find an approximate solution in the regime $g = (\frac{p}{6})^{1/2} \ll 1$

$${}_{+}^{\text{DFS}}(k) = \frac{1}{3} \frac{g}{2} \cos \frac{j}{\frac{1}{+}^{\text{DFS}}(k)} \ln \frac{j}{\frac{1}{+}^{\text{DFS}}(k)} = \frac{1}{3} \frac{g}{2} \sin \frac{j}{\frac{1}{+}^{\text{DFS}}(k)} \ln \frac{4}{j} \frac{4}{j + \frac{1}{k}}; \quad (2.19)$$

where $\frac{+}{k} = (\frac{+}{k} + \frac{D_{FS}}{+}(\frac{+}{k})^2)^{1/2}$. $\frac{D_{FS}}{+}(\frac{+}{k})$ is nearly constant near the Fermi surface ($\frac{+}{k} < \frac{D_{FS}}{+}(\frac{+}{k})$) and decreases for $\frac{+}{k} > \frac{D_{FS}}{+}(\frac{+}{k})$. This can be seen explicitly if one further approximates the above solution as

$$\frac{D_{FS}}{+}(\frac{+}{k}) = \frac{D_{FS}}{+}(\frac{+}{k}) \sin \left(\frac{g}{6} \ln \frac{\frac{+}{k}}{2} \right) \quad 0 < \frac{+}{k} < \frac{D_{FS}}{+}(\frac{+}{k}) \quad \frac{D_{FS}}{+}(\frac{+}{k}) < \frac{+}{k} \quad j : \quad (2.20)$$

The gap at the Fermi surface is determined as

$$\frac{D_{FS}}{+}(\frac{+}{k}) = 4 e^{-\frac{P}{3} \frac{g^2}{2} = g} : \quad (2.21)$$

The characteristic parametric dependence $\frac{D_{FS}}{+}(\frac{+}{k}) = e^{-c_{D_{FS}} g}$ with $c_{D_{FS}} = \frac{P}{3} \frac{g^2}{2}$ is obtained purely from the magnetic gluon. If one includes the contribution of the electric gluon, only the prefactor is modified as $\frac{D_{FS}}{+}(\frac{+}{k}) / (2 - m_D) e^{-c_{D_{FS}} g} = (2 - g) e^{-c_{D_{FS}} g}$. The coefficient $c_{D_{FS}}$ is smaller than that obtained from the Landau damping $c_{LD} = 3 \frac{g^2}{2} = \frac{P}{2}$. This implies that the Landau damping is a dominant effect of regulating the collinear singularity in the weak-coupling limit.

In a situation where $\frac{+}{k} \gg 1$, the gap equation can be cast into the following differential equation

$$k \frac{d^2}{dk^2} \frac{D_{FS}}{+}(\frac{+}{k}) + 3 \frac{d}{dk} \frac{D_{FS}}{+}(\frac{+}{k}) + \frac{g^2}{6} \frac{1}{k} \frac{D_{FS}}{+}(\frac{+}{k}) = 0; \quad (2.22)$$

where we have assumed that $\frac{D_{FS}}{+}(\frac{+}{k}) \neq 0$ as $k \gg 1$. The asymptotic solution of this equation for $g^2 < 3/2$ is

$$\frac{D_{FS}}{+}(\frac{+}{k}) / k ; = 1 + \frac{P}{1 - g^2/3} : \quad (2.23)$$

Therefore, in the weak coupling $g \ll 1$, the gap decreases slowly as $1/k^2$ for $k \gg 1$ and does not vanish for arbitrary large k . This long tail is a direct consequence of the gluonic interaction which allows scattering of quarks with an arbitrary energy-momentum transfer. Otherwise, the gap cannot take the nonzero value far away from the Fermi surface.

This is in sharp contrast to the gap in the standard weak-coupling BCS superconductivity in metals,³ where

$$\frac{BCS}{+}(p) = \begin{cases} \frac{+}{p} & p < !_D \\ 0 & \text{otherwise} \end{cases} \quad (2.24)$$

with p , $!_D$ and $!_D$ being the electron energy, the electron Fermi energy and the ultraviolet divergence cut-off of the phonon interaction originating from the lattice structure, respectively. As we mentioned above, the long tail in Eq. (2.23) is intimately related to the absence of the intrinsic ultraviolet-cuto-off such as $!_D$ in QCD.

D. Full gap equation

Now let us examine the structure of the full gap equation (2.6) which contains the effects of the Landau damping, the diffuse Fermi surface, the color-electric interaction and the antiquark pairing.

First we make a brief comment on the gauge-parameter dependence of the gap equation. Although physical quantities should be gauge invariant, special truncation scheme of the diagrams such as the ladder approximation introduces gauge-parameter dependence. It has been claimed that (i) $\frac{+}{k}$ is gauge invariant at extremely high density [8], and (ii) the gauge dependent contribution only begins to decrease at extraordinarily high densities $> 10^8$ MeV and seems to converge to the result of the Landau gauge ($\frac{+}{k} = 0$) [21]. We will show in Appendix A that, under the proper treatment of the diffuse Fermi surface, the $\frac{+}{k}$ -dependence survives in the gap equation for $\frac{+}{k}$ but gives

³This is a solution of the simplest gap equation discussed in the original BCS paper [13].

$$\frac{BCS}{+}(k) = \frac{1}{2} \sum_{k^0} X_{k,k^0} \frac{BCS}{+}(k^0) \frac{BCS}{+}(k^0) \frac{BCS}{+}(k^0)$$

where $X_{k,k^0} \neq 0$ for $!_D < k^0 < !_D + !_D$ and $X_{k,k^0} = 0$, otherwise.

a sub-leading contribution. Under this remark, we will take a standard choice $\epsilon = 0$ in the following to study the relative change of the momentum-dependent gap at high density and low density.

In Eq. (2.6), we adopt the static gluon propagator with the Debye screening (for the electric part) and the Landau damping (for the magnetic part). The imaginary part of the gap function will be neglected as we stated before. To take into account the higher order corrections to the quark-gluon vertex, which is in general momentum dependent, we replace the lowest order coupling g by the momentum dependent one $g(q; k)$ (see the discussion below for more details). Using the approximation $P^L \approx 0$ and performing the q_0 integration, the gap equation becomes

$$\begin{aligned}
 (k; k) &= \frac{Z}{dq q^2} \int_1^Z d(\cos \theta) \frac{g^2(q; k)}{12^2} \frac{q + (q; q)}{E_+^2 + j^2} \\
 &\quad + D_{MG}(q; k; q; k; \cos \theta) \frac{1}{2} \int_1^Z \frac{(q - q - k)(k - k - q)}{q^2 + k^2} \frac{!}{2qk \cos \theta} + D_{EL}(q; k; \cos \theta) \frac{1}{2} \frac{q - k}{2} \\
 &\quad + \frac{Z}{dq q^2} \int_1^Z d(\cos \theta) \frac{g^2(q; k)}{12^2} \frac{(q; q)}{E^2 + j^2} \\
 &\quad + D_{MG}(q; k; q; k; \cos \theta) \frac{1}{2} \int_1^Z \frac{(q - q - k)(k - k - q)}{q^2 + k^2} \frac{!}{2qk \cos \theta} + D_{EL}(q; k; \cos \theta) \frac{1}{2} \frac{q - k}{2} ;
 \end{aligned}$$

where the magnetic/electric gluon propagators $D_{MG} = D_{EL}$ are given by

$$D_{MG}(q; k; q_0; k_0; \cos \theta) = \frac{(q - k)^4}{(q - k)^2 + M^4 (q_0 - k_0)^2} + (q_0 ! - q); \quad D_{EL}(q; k; \cos \theta) = \frac{1}{(q - k)^2 + m_D^2}; \quad (2.25)$$

Performing the angular integration and making the redefinition $(k; k) = (k, k)$, we finally obtain

$$(k) = \int_0^{Z_1} dq V(q; k; q; k) \frac{!}{E_+ (q)^2 + j + (q)^2} + \int_0^{Z_1} dq V(q; k; q; k) \frac{!}{E (q)^2 + j + (q)^2}; \quad (2.26)$$

where,

$$\begin{aligned}
 V(q; k; q_0; k_0) &= \frac{g^2(q; k)}{48^2} \frac{q}{k} \frac{1}{3} \ln \frac{(k + q)^6 + M^4 (q_0 - k_0)^2}{(k - q)^6 + M^4 (q_0 - k_0)^2} + (q_0 ! - q) + f_{MG} \\
 &\quad + \frac{g^2(q; k)}{48^2} \frac{q}{k} \frac{(k - q)^2 + m_D^2}{2qk} \ln \frac{(k + q)^2 + m_D^2}{(k - q)^2 + m_D^2} + f_{EL} ;
 \end{aligned} \quad (2.27)$$

Here f_{EL} is just a constant, and f_{MG} is a rather complicated function of q and k . Since no singularity appears in $f_{EL, MG}$ when $m_D = 0, M = 0$ and $q = k = 0$ are taken, they are considered to be sub-leading contribution and will be neglected in the following analysis. In the definition of V , the first (second) term corresponds to the magnetic (electric) gluon contribution. We call the first integral in Eq. (2.26) as "quark-pole contribution" and the second integral as "antiquark-pole contribution", because $E_+ = q$ ($E = q + j$) is involved in the former (latter). Near the Fermi surface $q = 0$, the first integral in Eq. (2.26) gives the dominant contribution due to the small denominator $(E_+^2 + j^2)^{1/2} = f(q)^2 + j^2 g^{1/2} \approx 0$.

At extremely high density, the Cooper pairing is expected to take place only near the Fermi surface as we have discussed. In this case, we can safely neglect the antiquark-pole contribution for calculating $\langle \rangle$. Furthermore, one may replace the momentum dependent vertex by the coupling constant on the Fermi surface

$$g^2(q; k) = g^2(q = 0; k = 0); \quad (2.28)$$

If g is large enough, $g^2(q = 0; k = 0)$ may be identified with the standard running coupling

$$g^2(\theta) = \frac{8^2}{\theta} \frac{1}{\ln \frac{\theta^2}{Q^2 C_D}}; \quad (2.29)$$

where $\theta_0 = (11N_c - 2N_f) = 3$. Thus, keeping only the magnetic interaction, one recovers the gap equation (2.13) for g^2 with $g^2(\theta)$ in the weak-coupling limit.

At low densities, sizable diffusion of the Fermi surface occurs and the weak-coupling approximations leading to Eq. (2.13) are not justified. Therefore, we need to solve the coupled gap equations Eq. (2.26) numerically. In particular, the replacement Eq. (2.28) is not justified when q and k are not close to 0 . The contribution from the antiquark pole is also not entirely negligible.

As for the explicit form of $g^2(q;k)$, there exists a long history of research in connection with the Dyson-Schwinger equation for describing dynamical chiral symmetry breaking in QCD [22-24]. In the "improved ladder approximation" [22], $g^2(q;k)$ is taken to be

$$g^2(q;k) = \frac{8}{\pi} \frac{1}{\ln((p_{max}^2 + p_c^2)^{-2})}; \quad p_{max} = max(q;k); \quad (2.30)$$

where p_c^2 plays a role of a phenomenological infrared regulator, and π dictates the logarithmic decreases of the vertex at high momentum. The quark propagator in the improved ladder approximation in the vacuum is known to have a high momentum behavior consistent with that expected from the renormalization group and the operator product expansion. For the numerical values of π and p_c^2 , we adopt 400 MeV and 1.5^{-2} respectively. They are determined to reproduce the low energy meson properties for $N_f = 2$ by solving the Schwinger-Dyson equation for the quark propagator and the Bethe-Salpeter equation for the $q\bar{q}$ bound state in the vacuum [24].

E. Occupation number, correlation function and coherence length

To clarify the structural change of the color superconductor from high density to low densities, it is useful to examine the following physical quantities related to the gap function.

(i) The quark and antiquark occupation number in each momentum state: This is a fundamental quantity characterizing the usefulness of the Fermi surface. It is related to the diagonal (1-1) element of the quark propagator in the Nambu-Gorkov formalism

$$\begin{aligned} h_j^{ab}(t;y) i_i^a(t;x) i_{super}^b &= \lim_{x^0 \rightarrow y^0} i[S_{11}]_{ij}^{ab}(x-y)^0 \\ &= \frac{Z}{(2\pi)^3} \frac{d^3 q}{e^{iq(x-y)}} + (q) \left(\frac{1}{2} \right) + (q) (P_3^c)_{ab} (1_F)_{ij} \\ &+ \frac{1}{2} \left(1 - \frac{E_+(q)}{E_+(q)^2 + j_+(q)^2} \right) + \frac{1}{2} \left(1 + \frac{E_-(q)}{E_-(q)^2 + j_-(q)^2} \right) (1 - P_3^c)_{ab} (1_F)_{ij}; \end{aligned} \quad (2.31)$$

where P_3^c is a projection matrix to the third axis in the color space. From this expression, one can extract the quark and the antiquark occupation numbers as

$$n^{1,2}(q) = \frac{1}{2} \left(1 - \frac{E_+(q)}{E_+(q)^2 + j_+(q)^2} \right); \quad n_+^3(q) = (q); \quad n_-^3(q) = 0; \quad (2.32)$$

where the superscripts (1,2 and 3) stand for color indices. Since the third axis in the color space is chosen to break the color symmetry, quarks with the third color do not contribute to form Cooper pairs. When the gap is zero $\Delta = 0$, the system reduces to the ordinary quark matter with a sharp Fermi sphere; $n_+^{1,2}(q) = (q)$ and $n_-^{1,2}(q) = 0$.

(ii) The $q\bar{q}$ and $q\bar{q}$ correlation functions in the momentum space $\hat{n}(q)$ and in the coordinate space $n(r)$: They reflect the internal structure of the Cooper pairs in color superconductor. These correlations are related to the off-diagonal (1-2) element of the quark propagator:

$$\begin{aligned} h_i^a(t;x) h_j^b(t;y) i_{super} &= \lim_{x^0 \rightarrow y^0} i[S_{12}]_{ij}^{ab}(x-y) \\ &= \frac{Z}{(2\pi)^3} \frac{d^3 q}{e^{iq(x-y)}} \left(\frac{1}{2} \frac{+ (q)}{E_+(q)^2 + j_+(q)^2} + \frac{1}{2} \frac{+ (q)}{E_-(q)^2 + j_-(q)^2} \right) (i_5 C) (1_F)_{ij}^{ab}; \end{aligned} \quad (2.33)$$

$\hat{n}(q)$ is simply extracted from the above and $n(r)$ is defined as the Fourier transform

$$\hat{n}(q) = \frac{1}{2} \frac{+ (q)}{E_+(q)^2 + j_+(q)^2}; \quad n(r) = N \frac{d^3 q}{(2\pi)^3} \hat{n}(q) e^{iqr}; \quad (2.34)$$

where N is a normalization constant determined by $\int_0^R d^3r \mathcal{J}_+(r)^2 = 1$.

(iii) The coherence length ζ_c characterizing the typical size of a Cooper pair: It is defined simply as a root mean square radius of $\mathcal{J}_+(r)$:

$$\zeta_c^2 = \frac{\int_0^R d^3r r^2 \mathcal{J}_+(r)^2}{\int_0^R d^3r \mathcal{J}_+(r)^2} = \frac{\int_0^{R_1} dk k^2 \mathcal{J}_+^2(k) dk}{\int_0^{R_1} dk k^2 \mathcal{J}_+^2(k) dk} : \quad (2.35)$$

A measure of the coherence length ζ_c in the weak-coupling limit is known as the Pippard length, which is given by $\zeta_p = (1 + \gamma)^{-1}$ [25]. It is shown in Appendix B that the quark correlation $\mathcal{J}_+(r)$ in the weak-coupling limit behaves as

$$\mathcal{J}_+(r \gg 1) \sim \frac{\sin(r)}{(r)^{3/2}} e^{-r/\zeta_p} : \quad (2.36)$$

In a typical type-I superconductor in metals, the Pippard length is of the same macroscopic order $\zeta_p \sim 10^4$ cm, whereas inverse Fermi momentum is of the microscopic order $k_F^{-1} \sim 10^8$ cm. The inverse of the Debye cutoff is in between the two scales $\Lambda_D^{-1} \sim 10^6$ cm. Therefore there is a clear scale hierarchy, $\Lambda_D \ll k_F$. Because of the absence of the intrinsic scale Λ_D , similar scale hierarchy in QCD at extremely high density reads $e^{-\zeta_p} \ll 1$. At lower densities, however, such scale separation becomes questionable for ζ_p is not small.

III. NUMERICAL RESULTS

In this section, we present numerical results of the momentum-dependent gap and the other physical quantities. In Sect. IIIA, we show solutions of the gap equations at very high density. Then we discuss whether the result has similarity to that in the BCS superconductivity for metals [see Eq. (2.24)]. What makes the color superconductor unique is the absence of the intrinsic cutoff scale Λ_D . Nevertheless, we will see that similar relation as Eq. (2.24) holds under the replacement $\Lambda_D \rightarrow 0$ at least at extremely high density. We will also examine how the results of the gap equation in the weak-coupling limit (2.13) are modified when the effects such as the color-electric interaction, the momentum-dependent coupling and the antiquark-pole contribution are taken into account.

In Sects. IIIB and IIIC, we repeat the same calculations at lower densities and show a qualitative difference from the weak-coupling limit. Substantial modification of the Fermi surface at low densities will be explicitly shown by computing the occupation number. Quark correlation in the color superconductor and the size of the Cooper pair are calculated in Sect. IIID. The results indicate that the color superconductivity at low densities is no longer similar to the usual BCS-type superconductivity.

In Sects. IIIA and IIIB, starting from the simplest gap equation in the weak-coupling limit (2.13), we will include the contributions of color-electric interaction, momentum-dependent coupling and antiquark-pole, step by step. This procedure clarifies the importance of each contribution. Let us define each step below, for later convenience.

Step 1: We solve the gap equation for Δ_+ in the weak-coupling limit Eq. (2.13). Un-screened color-magnetic interaction ($M^2 = 0$) and the momentum-independent coupling $g^2(\vec{q})$ are used in this step.

Step 2: We switch on the Landau damping of the color-magnetic interaction in Eq. (2.13) treated in Step 1.

Step 3: The Debye-screened color-electric interaction is further taken into account in Step 2. This corresponds to solving Eq. (2.26) for Δ_+ with neglecting the antiquark-pole contribution and with making a replacement $g^2(q; k) \rightarrow g^2(\vec{q})$.

Step 4: Same as Step 3 except for the use of $g^2(q; k)$ instead of $g^2(\vec{q})$ for the vertex.

Step 5: The antiquark-pole contribution is also taken into account in Step 4. This gives the complete solution of our full coupled gap equations Eq. (2.26).

Throughout the all steps, g^2 in the Debye screening mass Λ_D is taken to be $g^2(\vec{q})$ for simplicity. In Step 4 and Step 5, we use a phenomenological value $\gamma = 400$ meV and $p_c^2 = 1.5^2$ for $g(q; k)$ as we have already mentioned in Sect. IIID.

A. Momentum dependence of the gap at high density

In this subsection, we solve the gap equations at chemical potential $\mu = 2^{12} \approx 1.6 \text{ TeV}$. This corresponds to the baryon density $\rho_B = 1.1 \times 10^{11} \text{ fm}^{-3}$ with $\rho_0 = 0.17 \text{ fm}^{-3}$ being the normal nuclear matter density. At this extremely high density, we expect that the full gap equation Eq. (2.26) is well approximated by its weak-coupling limit, Eq. (2.13). Furthermore, the analytic solution Eq. (2.15) is expected to give a fair approximation of Eq. (2.13) around the Fermi surface.

Step 1:

The dashed line in Fig. 1(a) shows the numerical solution of Step 1. Several remarks are in order in relation to this result.

First of all, the result has a very narrow peak at the Fermi surface as we anticipated. The height of the peak, $\Delta(k=0)$, is consistent with the analytic result $\Delta_{\text{DFS}}(0) \approx 33 \text{ MeV}$ estimated in Eq. (2.21). The peak is not a singular one, but has a plateau with the width of $2\Delta(k=0)$, which is also consistent with the analytic solution Eq. (2.19). This is explicitly shown in Fig. 1(b), where we compare the numerical result and the analytic solution just around the Fermi surface. The similar plateau structure is also seen in the frequency dependence of the gap as discussed in Ref. [7] because of the reason we have discussed below Eq. (2.18).

Secondly, the decrease of the gap at high momentum k also agrees with the analytic solution Eq. (2.23). Such a long tail is due to the unscreened nature of the color-magnetic interaction and is quite different from the behavior of the gap in the standard BCS-type superconductivity.

Thirdly, the global structure of the gap in Fig. 1(a) is not symmetric with respect to the Fermi surface. In fact, the gap deep inside the Fermi sphere is not negligible. This does not contradict the analytic solution (2.19) because we have used approximation valid only in the vicinity of the Fermi surface in deriving the solution. Clearly, the gap equation Eq. (2.17) (as well as Eq. (2.13)) is not symmetric under the exchange $k \leftrightarrow -k$. The value $\Delta(k=0)$ in Step 1 is extracted from Eq. (2.17) by approximating the kernel as $\ln j(k+q) = (k+q)j - 2k=q$ for small k . One then finds

$$\Delta_{\text{DFS}}(k=0) \approx \frac{g^2}{6^2} \int_0^1 dq \frac{\Delta_{\text{DFS}}(q)}{(q^2 + \Delta_{\text{DFS}}(q)^2)^{1/2}};$$

Assuming that the dominant contribution of the above integral comes from the region $q \ll 1$, one may use the approximate solution Eq. (2.20) to evaluate this integral. The result is

$$\Delta_{\text{DFS}}(k=0) \approx (g=6)^2 \left(2 \ln \left(\frac{p}{2} + 1 \right) + 4 \frac{p}{3} \right) = \Delta_{\text{DFS}}(0);$$

where we ignored the contribution from $3 < q < 1$, which is higher order in $\Delta_{\text{DFS}}(0)$. For $\mu = 2^{12}$, we find $\Delta_{\text{DFS}}(0) = \Delta_{\text{DFS}}(0) \approx 0.39$. This value is consistent with the ratio 0.26 of the numerical result in Fig. 1(a). The above approximation for the kernel does not hold for large k ; this is the reason why the gap is asymmetric between $k \approx 0$ and $k \approx \mu$.

Step 2:

The solid line in Fig. 1(a) is the result of Step 2 where the Landau damping is added to Step 1. Comparing the solid and dashed lines, one finds that the magnitude of the gap with the Landau damping is almost 10^{-2} of that with DFS alone. This suppression factor can be estimated from the analytic solutions in Sect. II C where we have solved the gap equation with the DFS effect alone and that with the Landau damping alone. The predicted value of the gap at $\mu = 2^{12}$ in the analytic solutions are $\Delta_{\text{DFS}}(0) = 33 \text{ MeV}$ and $\Delta_{\text{LD}}(0) = 0.22 \text{ MeV}$. Also this is an explicit demonstration of the argument discussed in Sect. II B: namely the Landau damping is much more effective than the direct Fermi surface in regulating the collinear singularity near the Fermi surface.

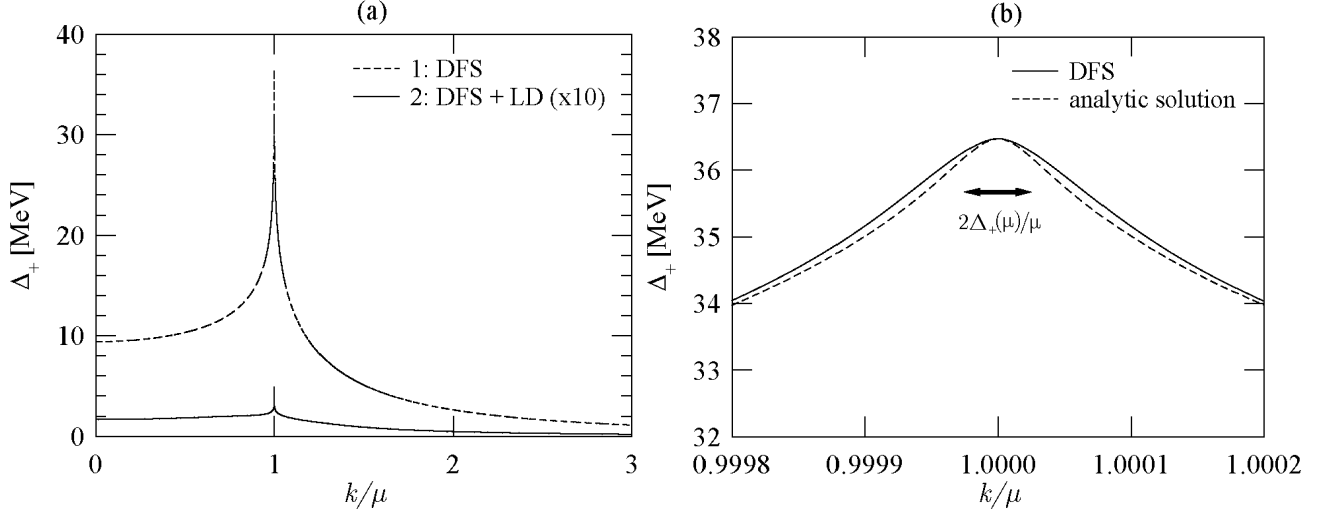


FIG. 1. (a) The momentum dependence of the gap in Step 1 and Step 2 at extremely high density, $\mu = 2^{12} \text{ MeV} = 1.6 \text{ TeV}$. The dashed line (Step 1) is a solution of the gap equation without the Landau damping Eq. (2.17). The solid line (Step 2) is a solution of the gap equation with the Landau damping Eq. (2.13). The magnitude of the latter is multiplied by 10 in the figure. In both cases, only the magnetic interaction is taken into account and the momentum independent vertex $g^2(0)$ is used. (b) The gap in Step 1 plotted around the Fermi surface. The solid line is the numerical result and the dashed line is the analytic solution Eq. (2.19) normalized to the numerical result at the Fermi surface.

Step 3:

To study the effect of color-electric interaction, let us move on to Step 3. In Fig. 2 (a), comparison is made between the gap with the magnetic interaction alone (the dashed line, same as the solid line in Fig. 1 (a)) and the gap with both magnetic and electric interactions (the solid line). The electric interaction induces a large enhancement (about 10 times) of the gap almost independently of momentum.

This enhancement may be understood in a qualitative manner. In the coordinate space, the Debye-screened electric interaction behaves as a Yukawa potential. Such a short-range interaction can form only a loosely bound Cooper pairs with a large size. In fact, if one solves the gap equation with the electric interaction alone, one finds a very small gap compared to the one in Fig. 2 (a). The situation becomes different when the magnetic and electric interactions coexist: Small size Cooper pairs are formed primarily by the long-range magnetic interaction. Then, even the short-range electric interaction becomes effective to generate further attraction between the quarks. This cooperative effect can qualitatively explain the reason why addition of the electric interaction enhances the gap.

Now, let us try to understand the magnitude of the enhancement quantitatively. In the analytic studies in Sect. II C, we found that addition of electric interaction changes the prefactor of the gap at the Fermi surface and indeed enhances the gap. The enhancement factors at the Fermi surface are $8^3 = 512$ for $\text{LD}(\mu)$, and $2 = g^2 = 6.3$ for $\text{DFS}(\mu)$ at $\mu = 2^{12} \text{ MeV}$. The numerical enhancement factor (~ 10) in Fig. 2 (a) lies just in between these values.

Step 4:

To see the effect of the momentum dependent vertex $g^2(q; k)$, let us compare the dashed line in Fig. 2 (b) (where $g^2(q; k)$ is used) with the solid line in Fig. 2 (a) (where $g^2(0)$ is used). Since $g^2(q; k)$ works as a weight factor in the momentum integral in the gap equation, substantial difference should appear between the two cases if the contribution away from the Fermi surface is not negligible in the integral. However, we find no significant difference between the two cases at high density in Fig. 2. This implies that the color superconductivity at high density is governed by the physics near the Fermi surface.

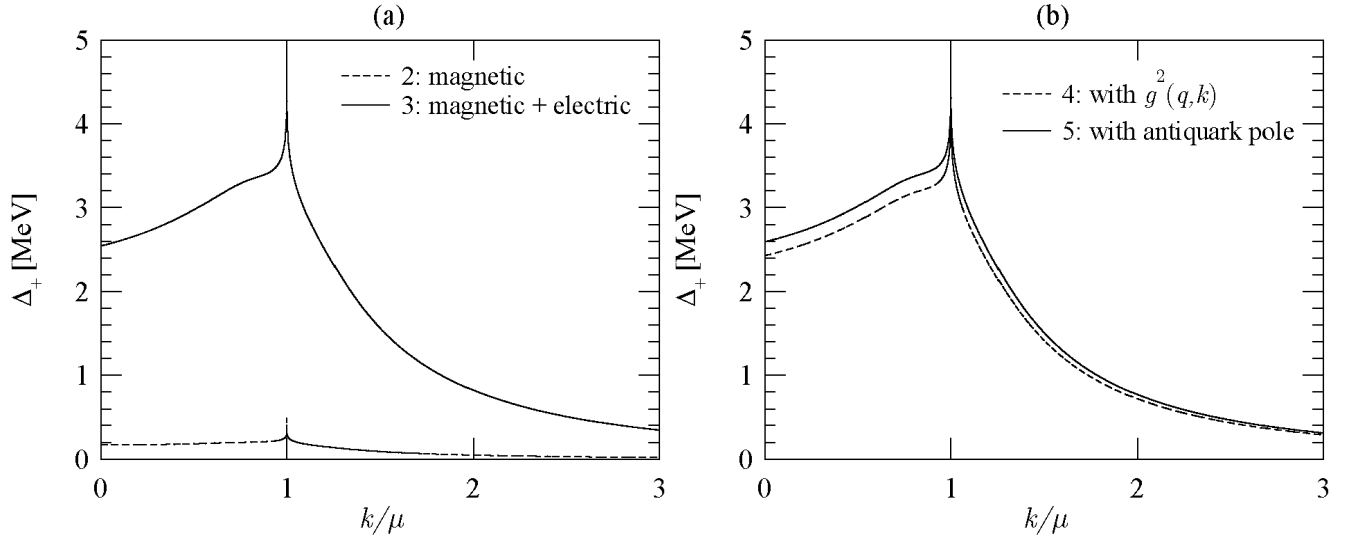


FIG. 2. The momentum dependence of the gap from Step 2 through Step 5 at high density, $\mu = 2^{12}$. (a) Comparison of Step 2 and Step 3: The dashed line (= the solid line in Fig. 1(a)) is a result of the magnetic interaction alone (Step 2). The solid line is the gap with both magnetic and electric interactions included (Step 3). (b) Comparison of Steps 4 and 5: The dashed line is the gap in which the momentum dependent vertex $g^2(q; k)$ is used (Step 4) instead of the momentum independent coupling $g^2(0)$ (Step 3). The solid line is the gap as a solution of the full gap equation with $g^2(q; k)$ and the antiquark pole (2.26).

Step 5:

Let us examine the last stage, Step 5, where the antiquark-pole contribution is included. In this case, the gap equation is a coupled equation for Δ_+ and Δ_- . The solid line in Fig. 2(b) is $\Delta_+(k)$ obtained by solving the full coupled gap-equation (2.26). This should be compared with the dashed line in Fig. 2(b) in Step 4. Since the antiquark-pole contribution enhances the gap only slightly, we can conclude that the quark-pole dominance is indeed a good approximation at very high density.

In Fig. 3, we compare the solutions of the full gap equation (2.26) in Step 5. Δ_+ in this figure is the same as the solid line in Fig. 2(b). The gap in the antiquark channel Δ_- is a smoothly decreasing function of the momentum. Although Δ_- is not small compared to Δ_+ , it does not imply that the sizable antiquark Cooper pairs exist in the system because the number of antiquarks are much smaller than quarks as we will show in Sect. III D.

Finally, Fig. 4 shows a comparison between the momentum dependence of the numerical solution Δ_+ in Step 5 (the solid line which is the same as the solid line in Fig. 3) with the analytic solution near the Fermi surface (2.15) (the dashed line). The peak height of the analytic solution is adjusted so that the solid and dashed lines coincide at $k = 0$. In the vicinity of the Fermi surface, the momentum dependence of the analytic solution agrees with the numerical solution very well, while the deviation becomes considerable away from the Fermi surface. Note that the coincidence at $k = 0$ is accidental because the analytic result (2.15) is valid only near the Fermi surface.

In this subsection, we have solved the momentum-dependent gap equations at high density $\mu = 2^{12}$ from Step 1 through Step 5. The characteristic features of the momentum-dependent gap are (i) there is a sharp peak at the Fermi surface, and (ii) the gap decays rapidly but is nonzero for momentum far away from the Fermi surface. The property (i) is similar to the standard BCS superconductivity [see Eq. (2.24)] but (ii) is not, due to the absence of intrinsic ultraviolet divergence of the gluonic interaction in QCD. As for the magnitude of the gap at high density, the Landau damping (the color-electric interaction) reduces (enhances) the gap considerably. The effects of the momentum-dependent vertex $g^2(q; k)$ and the antiquark pairing are shown to be not important at high density. Thus global shape of the gap as a function of spatial momentum is essentially determined by the simplified gap equation (2.13).

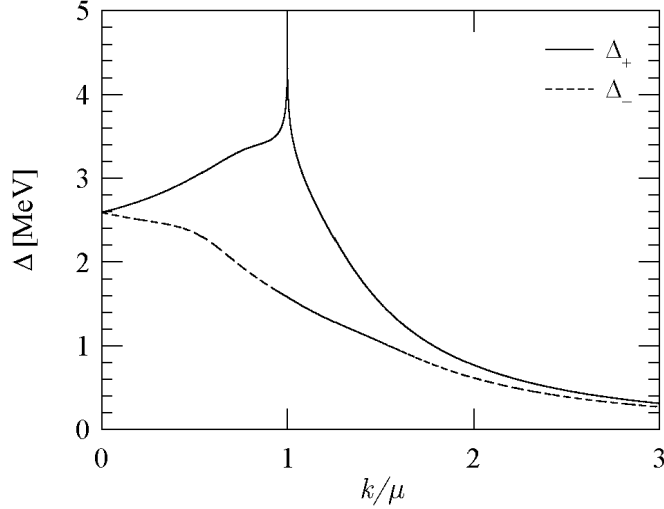


FIG. 3. Δ_+ and Δ_- in the full coupled gap equation in Step 5 at high density, $\mu = 2^{12}$.

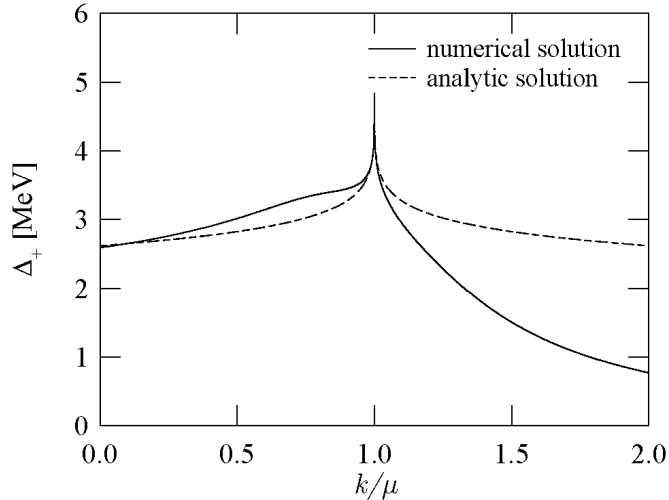


FIG. 4. Comparison of the numerical solution of Δ_+ in Step 5 (the solid line) and the analytic solution near the Fermi surface (the dashed line) at high density, $\mu = 2^{12}$. The latter is normalized to the former at $k = 0$.

B. Momentum dependence of the gap at low density

In this subsection, we carry out the same calculations as in Sect. IIIA at lower density $\mu = 2 = 800$ MeV (which corresponds to the baryon density $n_B = 132_0$). Then we discuss the difference between the two cases.

Steps 1 and 2:

Results of Steps 1 and 2 are shown in Fig. 5. By comparing the solution without the Landau damping at low density (the dashed line in Fig. 5) and at high density (the dashed line in Fig. 1(a)), we find two qualitative differences. The first one is the absence of a sharp peak at low density. The width of the peak in Fig. 5 in terms of k is much wider than that in Fig. 1(a). The second difference is the larger asymmetry of the gap at low density with respect to the Fermi surface $k = 0$. These features may be attributed to the larger coupling at low density, $g(\mu = 2) = g(\mu = 2^{12}) = 3.09 = 0.99 = 3.12$. Because of this large interaction strength, the Cooper pairs far from the Fermi surface are easily formed and the physics of superconductivity is no longer limited on the Fermi surface.

Shown by the solid line in Fig. 5 is the result with the Landau damping (Step 2). The dynamical screening effect reduces the magnitude of the gap by a factor 4–5, which indicates the importance of Landau damping even at low densities.

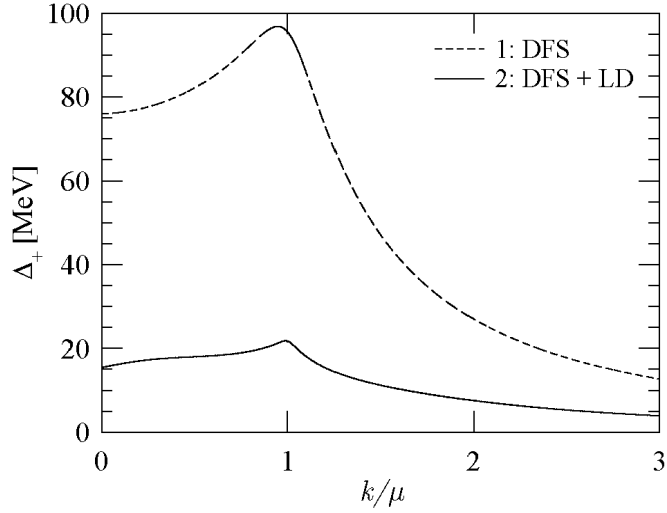


FIG. 5. Same as Fig. 1 except that the density is lower $\rho = 2 = 800$ MeV.

Steps 3 and 4:

Comparing the dashed line (with the magnetic interaction alone) and the solid line (magnetic and electric interactions) in Fig. 6(a), we again find that the addition of the color-electric interaction induces a large enhancement of the gap of a factor 3–4.

The result of Step 4 (where $g^2(q; k)$ is used) is shown as the dashed line in Fig. 6(b), which should be compared with the solid line in Fig. 6(a) where $g^2(\vec{q}; \vec{k})$ is used. In contrast to the high density case in Fig. 2(b), the momentum-dependent vertex makes the magnitude of the gap considerably smaller. This is one of the evidences that the momentum integration is not anymore dominated by the small region near the Fermi surface. The reason why the suppression of the gap takes place instead of the enhancement is understood as follows. Consider the gap at the Fermi surface $\Delta_+(k = 0)$. In the momentum integration of the gap equation Eq. (2.26) at $k = 0$, $g^2(q; k = 0) < g^2(\vec{q}; \vec{k})$ for $|\vec{q}| < q$, while $g^2(q; k = 0) = g^2(\vec{q}; \vec{k})$ for $|\vec{q}| > q$. Therefore, the momentum-dependent coupling always acts to reduce the magnitude of the integral as compared to the momentum-independent one.

Step 5:

To see the effect of the antiquark-pole contribution, Δ_+ as a solution of the full gap equation with (without) the antiquark pole (2.26) is shown in Fig. 6(b) by the solid (dashed) line. The antiquark-pole contribution enhances the gap by 10%. The difference between the solid and dashed lines in Fig. 6(b) is not huge but the absolute magnitude of the enhancement is larger than that in the extremely high density case shown in Fig. 2(b).

The reason for this enhancement is clear: As one decreases density, the quark Fermi sphere shrinks and the position of antiquark-pole at $k' = 0$ gets closer to the quark-pole $k' = 0$. Therefore, the antiquark-pole contribution becomes non-negligible. This also suggests that the more low-momentum antiquarks are present at low density which will be confirmed in Sect. III D by computing the occupation number of antiquarks.

Finally, in Fig. 7, we compare the quark-gap Δ_+ (the solid line) and the antiquark gap Δ_- (the dashed line). As in the case of high density, the antiquark gap Δ_- is a smooth function of k and is not small compared to Δ_+ .

In this subsection, we found that the momentum dependence of the gap at low density is quite different from that at very high density. The sharp peak at the Fermi surface disappears. The gap equation in the weak-coupling limit (2.13) is no longer a good approximation and all the contributions neglected in the weak-coupling limit are not negligible. All these results allow us to conclude that the color superconductivity at low density is not a phenomenon just around the Fermi surface. In subsections III D and III E below, we will strengthen this picture by looking at other quantities such as the quark occupation numbers and the size of the Cooper pair.

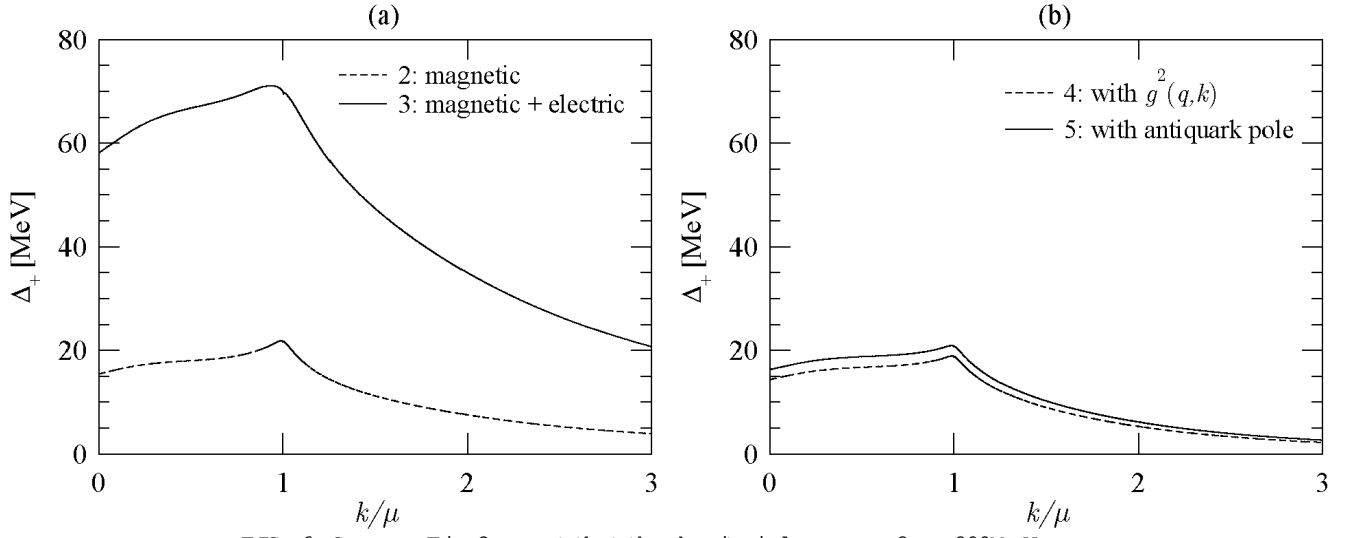


FIG. 6. Same as Fig. 2 except that the density is lower, $n = 2 = 800M$ eV.

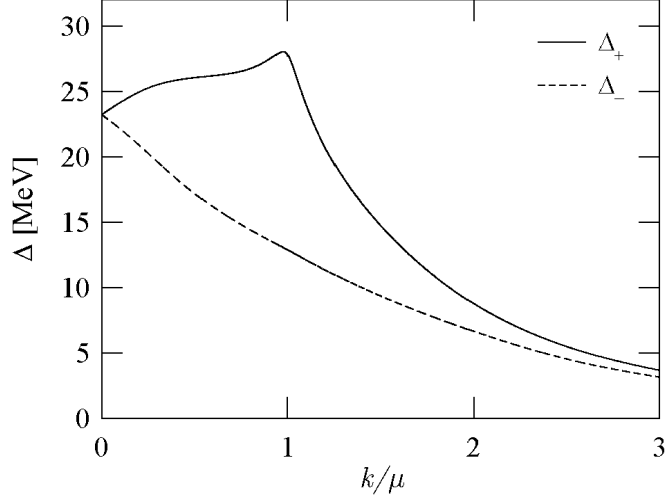


FIG. 7. Same as Fig. 3 except that the density is lower, $n = 2 = 800M$ eV.

C. Density dependence of the gap

Let us now examine how the gap at high density with a sharp peak changes into the gap at low density with only a broad bump. In Fig. 8, we show the gap $\Delta_+(k)$ as a solution of the full gap equation (Step 5) for a wide range of densities. Since the actual position of the Fermi surface moves as we vary the density, we use $k =$ as a horizontal axis in the figure in order to show the change of the global behavior. The figure shows that the sharp peak at high density gradually gets broadened and simultaneously the magnitude of the gap increases as we decrease the density.

In Fig. 9, the gap at the Fermi surface $\Delta_+(k)$ is shown as a function of the chemical potential. It decreases monotonically as μ increases, but turns into an increase for $\mu > 10^6$ M eV. The analytic solution $\Delta_+^{LD}(k)$ is also shown in Fig. 9. The magnitude of the analytic solution is normalized to the numerical solution at the highest density $\mu = 2^{12} \approx 1.6 \times 10^6$ M eV. At high density, the μ -dependence of the numerical result is in good agreement with the analytic form which has a parametric dependence $\Delta_+ / g^5 \propto \exp(-3\mu^2/2g)$ with $g^2 = g^2(0)$. On the other hand, the difference of the two curves at low density implies the failure of the weak-coupling approximation. As we have seen before, the use of $g^2(q, k)$ and the antiquark-pole has non-negligible effects on the gap in the low density regime.

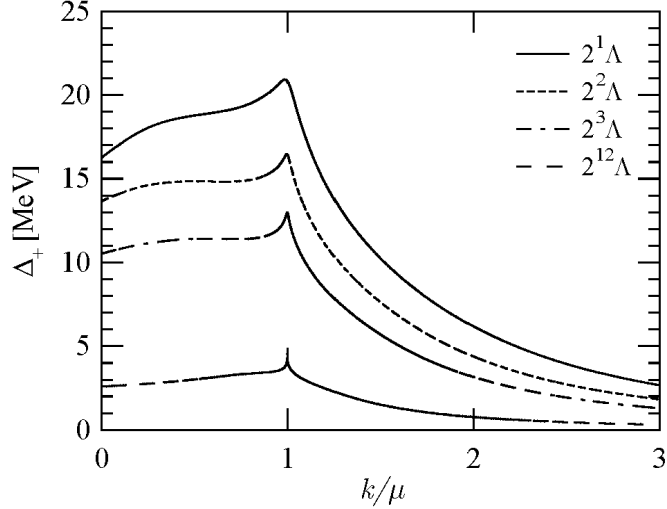


FIG. 8. Δ_+ (k) as a function of k/μ for various densities $\rho = 2^n$ with $n = 1, 2, 3, 12$. All the calculations are done with the momentum dependent vertex $g^2(q; k)$ and with the antiquark-pole contribution.

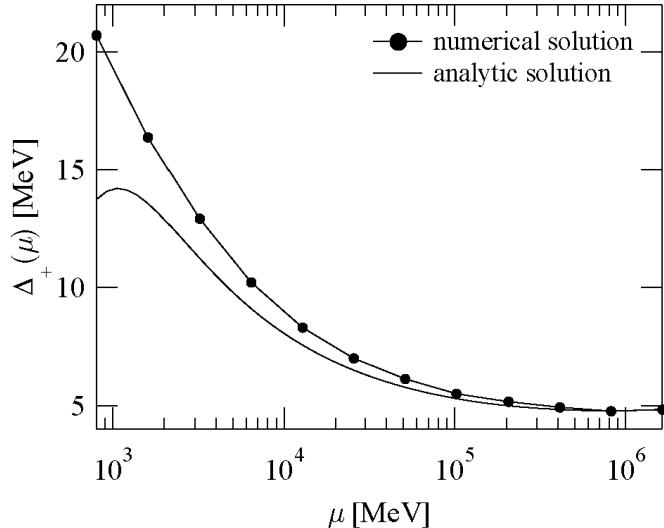


FIG. 9. Chemical potential dependence of the gap Δ_+ (μ) in the full calculation compared with the analytic result Δ_+^{LD} (—) normalized at the highest density $\rho = 2^{12}$.

D. Occupation numbers

So far we have seen that the weak-coupling picture of the color superconductivity is modified at low densities. In order to see how the Fermi surface is divided by the Cooper pairing, let us evaluate the occupation numbers of quarks and antiquarks. Since we have solved the full gap equation (2.26) for Δ_+ (k), we can immediately obtain the occupation numbers using Eq. (2.32).

In Fig. 10, the occupation numbers of quarks [Fig. 10(a)] and antiquarks [Fig. 10(b)] are shown at high density $\rho = 2^{12}$ and at lower densities $\rho = 2, 2^2$. One finds that the quark occupation numbers is almost a step function at high density, while it is smeared out for a wide region of momentum at low densities. The divisibility of the Fermi surface is found to be of the order of Δ_+ (k), which is consistent with the definition in Eq. (2.32).

Figure 10(b) implies that a small amount of the antiquarks also participate in the color superconductivity. Although the antiquark gap Δ_- is of the same order of the quark gap Δ_+ , the antiquark occupation number is generally suppressed due to the large energy denominator $f(k_+)^2 + j_-^2 g^{1=2}$. As one decreases the density, however, such suppression is relatively weakened and the magnitude of the antiquark occupation number increases, as can be seen from Figure 10(b).

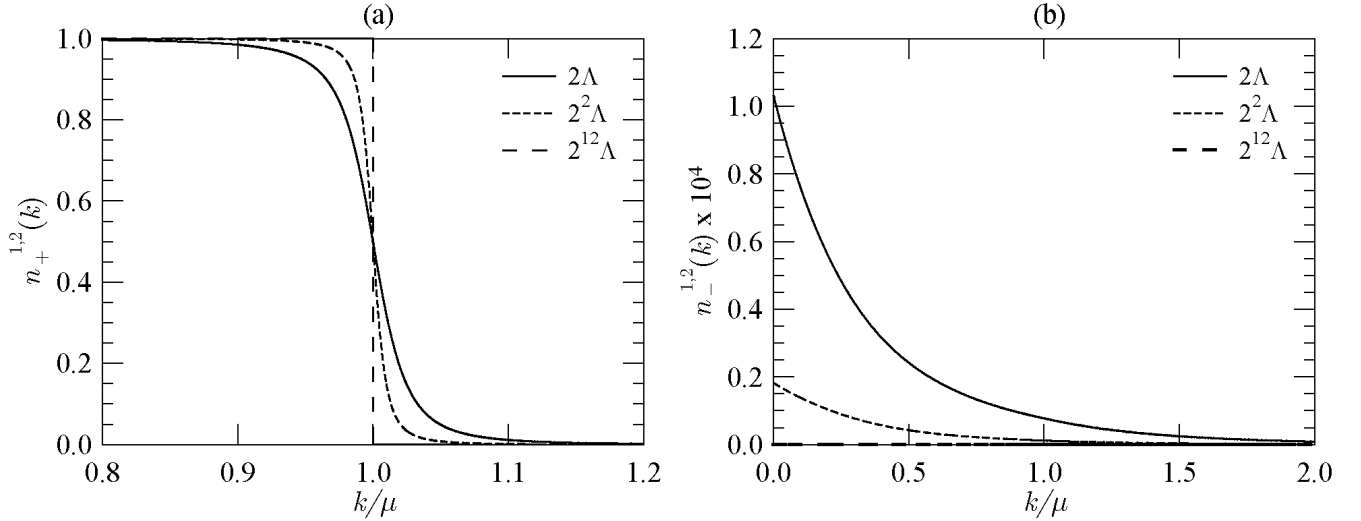


FIG. 10. Occupation numbers of quarks $n_+^{1,2}$ (a) and antiquarks $n_-^{1,2}$ (b) for several different densities.

E. Correlation function and coherence length

One of the advantages of treating the momentum dependent gap is that we are able to calculate the correlation function which physically corresponds to the "wavefunction" of the Cooper pair. Such correlations have been first studied in Ref. [15] in the context of the color superconductivity.

Using Eq. (2.34), we calculate the correlation functions of quarks and antiquarks, $\hat{\varphi}(k)$. The results at various densities are shown in Fig. 11. For quarks [Fig. 11 (a)], the correlation function at very high density has a sharp peak at the Fermi surface but it becomes broader as we decrease the density. This is of course due to the broadening of the gap which we found in Fig. 8.

For antiquarks [Fig. 11 (b)], the correlation is much weaker than that of quarks and is a smoothly decreasing function of k . Also, the magnitude of the correlation increases as we decrease the density. Since $\hat{\varphi}(k)$ holds for densities considered in this paper, the above features can be simply understood by an approximate relation, $\hat{\varphi}(k) \approx 2(k + \mu)$.

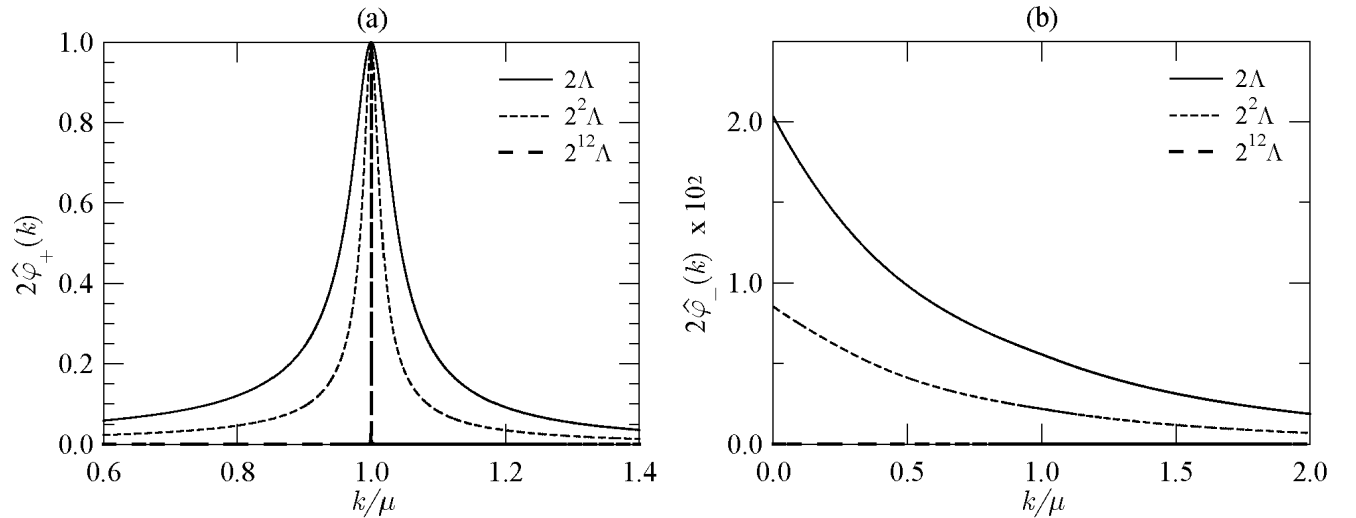


FIG. 11. The correlation functions in the momentum space at several different densities for quarks (a) and for antiquarks (b).

We can compute the size of a Cooper pair from the correlation function. Figure 12 (a) shows the coherence length ζ of a quark Cooper pair defined as the root mean square radius of the correlation function [see Eq. (2.35)]. The size of a Cooper pair becomes smaller as we go to lower densities. This tendency is understood by the behavior of the

Pippard length $\xi_p = 1 = \dots + (\dots)$ (which gives a rough estimate of the coherence length) together with the behavior of $\xi_c = \dots + (\dots)$ shown in Fig. 9.

Also, the Cooper pair becomes smaller as increases density beyond $\mu = 2^{12}$. However, it does not necessarily imply the existence of tightly bound Cooper pairs. In fact, the size of the Cooper pair makes sense only in comparison to the typical length scale of the system, namely the averaged inter-quark distance d_q defined as⁴

$$d_q = \frac{2}{2} \frac{1}{2}^{1=3} \dots$$

As we go to higher densities, the ratio ξ_c/d_q increases monotonically as shown in Fig. 12 (b). Namely loosely bound Cooper pairs similar to the BCS superconductivity in metals are formed at extremely high densities.

At the lowest density in Fig. 12 (b), the size of the Cooper pair is less than 4 fm and the ratio ξ_c/d_q is less than 10. The transition from $\xi_c/d_q \approx 1$ to $\xi_c/d_q \gg 1$ as μ decreases is analogous to the transition from the BCS-type superconductor to the so-called "strong coupling" superconductor. The weak-coupling BCS superconductivity may smoothly change into the Bose-Einstein condensation (BEC) of tightly bound Cooper pairs as the coupling strength increases [26]. Our result here suggests that the quark matter possibly realized in the core of neutron stars may be rather like the BEC of tightly bound Cooper pairs.

For better understanding of the internal structure of the quark Cooper pair, let us consider the correlation function in the coordinate space. Fig. 13 shows the spatial correlation of a Cooper pair at various chemical potentials normalized as $d^3 r f_+(r) f_-(r) = 1$: As is expected, the density dependence of the quark correlation in the coordinate space is opposite to that in the momentum space. At high density, most of the quarks participating in forming a Cooper pair have the Fermi momentum $k_F = \dots$ giving a sharp peak in the momentum space correlation. In the coordinate space, this corresponds to an oscillatory distribution with a wavelength $\lambda = 1 = \dots$ without much structure near the origin. (The oscillation is also evident from the factor $\sin(\lambda r)$ in the approximate correlation function Eq. (2.36) discussed in Sect. III E.) At lower densities, accumulation of the correlation near the origin in the coordinate space is much more prominent in Fig. 13. This implies a localized Cooper pair composed of quarks with various momentum. This is also seen by the broad momentum correlation in Fig. 11 (a).

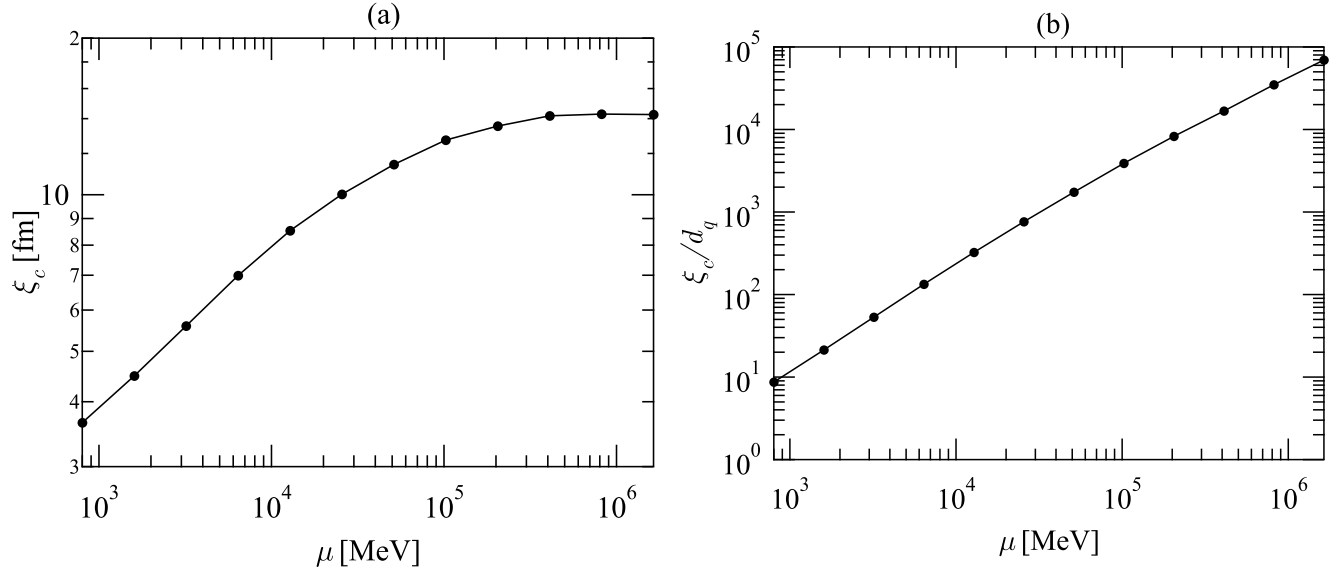


FIG. 12. (a): Density dependence of the coherence length. (b): Ratio of the coherence length ξ_c and the average inter-quark distance d_q as a function of the chemical potential.

⁴This is a result of free quarks. To obtain accurate density μ and d_q , we have to include contributions from interaction. However, such correction is suppressed by the power of $\mu = \dots$.

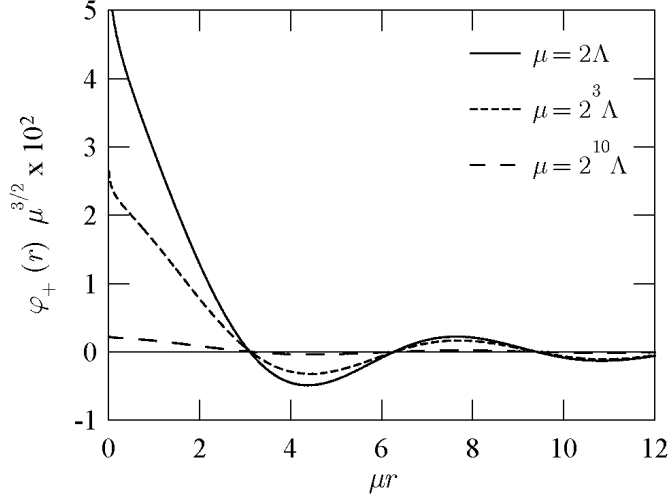


FIG. 13. The quark-quark correlation function $\varphi_+(r)$ in the coordinate space $\varphi_+(r)$ for several different chemical potentials. $\varphi_+(r)$ is normalized to be unity.

IV. SUMMARY AND DISCUSSION

In this paper, we have studied the spatial momentum dependence of a superconducting gap and the structure of the Cooper pairs in two-flavor color superconductivity. Nontrivial momentum dependence of the gap manifests itself at low densities, where relatively large QCD coupling allows the Cooper pairing to take place in a wide region around the Fermi surface. Our results imply that the quark matter which might exist in the core of neutron stars or in the quark stars could be rather different from that expected from the weak-coupling BCS picture.

Following is the summary of what we have discussed in this paper.

- (1) At high density, the weak-coupling gap equation with the electric and magnetic gluons is a good approximation. The momentum-dependent quark-gluon vertex and the coupling to the antiquark pairing do not change the weak-coupling result. The gap $\varphi_+(k)$ has a peak around the Fermi surface with a width $\sim 2\pi/(k)$ and decreases rapidly as k goes away from the Fermi surface. This is consistent with the analytic solution of the gap equation in the weak-coupling limit. All the results indicate that the Cooper pairing takes place only in a small region around the Fermi surface.
- (2) At lower density, the weak-coupling gap equation is no longer a good approximation. The momentum-dependent vertex and the coupling to the antiquark pairing have non-negligible effects. The sharp peak at the Fermi surface disappears. These imply that a large number of Cooper pairs away from the Fermi surface participate in the color superconductivity. This was confirmed by the quark occupation numbers and the quark-quark correlation. Therefore, color superconductivity at low density is not a phenomenon in the vicinity of the Fermi surface, but is a phenomenon with large modification of the Fermi surface.
- (3) The qualitative change of color superconductivity from high density to low density can be explicitly seen by the ratio of the size of the quark Cooper pair to the averaged inter-quark distance. At high density, the ratio is very large (about 10^5 at $\sim 10^6$ MeV) which is consistent with the standard BCS-type superconductivity. At lower densities, however, the ratio becomes small (about 10 at ~ 800 MeV). This situation is rather similar to the "strong coupling" superconductor which could be described by a Bose-Einstein condensate of tightly bound Cooper pairs.

There are several future problems.

Firstly, there are still several corrections to our "full" gap equation. They include the full hard-dense-loop corrections and the Meissner effect in the gluon propagator, and also the use of the plasmon dispersion in the diagonal self-energy of the quark propagator. The latter effect induces only a sub-leading change on the gap at the Fermi surface at high density [12,27], but may have non-negligible effects at lower densities. For treating both the diagonal and off-diagonal parts of the quark self-energy, the standard Eliashberg formalism must be used [28,13]. If we include all the above effects, the gap equation with frequency and momentum as independent variables should be solved [29].

Secondly, we assumed that there is no significant vacuum effects in the present paper. If the density is close to the critical density of chiral symmetry breaking, one must consider the interplay between the quark-antiquark condensate

and the quark-quark condensate [17,18,30]. This also requires us to treat the diagonal and off-diagonal components of the fermion self-energy simultaneously, which corresponds to the Hartree-Fock-Bogoliubov theory in many-body problem [31].

Thirdly, we have taken the Landau gauge $\gamma = 0$ in this paper. As we discussed in Sect. IID and in Appendix A, the γ -dependence in the gap equation remains as far as the direct Fermi surface is considered. Although it is a sub-leading contribution relative to the leading electric and magnetic interactions, it is desirable to develop a gauge invariant formalism especially when one treats the low density region.

Lastly, it will be very intriguing to find a new way of describing color superconductivity at low densities. The small size Cooper pairs with coherence length comparable to the inter-quark distance suggests that BEC description may be useful as in the analogous example in condensed matter physics. An analysis along this line has been discussed in Ref. [5] using the linear sigma model for the diquark field.

ACKNOWLEDGMENTS

H.A. would like to thank T. Tatsumi for his useful comments at the early stages of the work. He is also thankful to K. Suzuki for his various supports. K.I. is grateful to R. Pisarski, D. Rischke, T. Schäfer, and D.T. Son for their critical comments and suggestions. H.A. and K.I. are thankful to M. Matsuzaki for discussion. Lastly, H.A. and T.H. acknowledge V.A. Miransky for his interests in the work.

APPENDIX A : GAUGE DEPENDENCE OF Δ_+

In this Appendix, we discuss the gauge parameter dependence of the gap equation for Δ_+ at high density. We write the gauge dependent contribution to the gap equation for $\Delta_+(k)$ as $I(k)$. Neglecting the antiquark pole, it becomes

$$I(k) = \frac{g^2}{24^2} \int_0^{Z_1} dq \int_1^{Z_1} d\cos \theta \frac{p_+^2(q)}{E_+(q)^2 + p_+^2(q)^2} K(q; k; \cos \theta); \quad (A1)$$

where $\hat{q} \cdot \hat{k} = \cos \theta$ and K is defined as

$$K(q; k; x) = \frac{2qk}{q^2 + k^2} \frac{2qk \cos \theta}{2qk \cos \theta} \frac{(q - k \cos \theta)(k - q \cos \theta)}{q^2 + k^2} \frac{1 - \cos \theta}{2} : \quad (A2)$$

$I(k)$ should be added to the right hand side of (2.26) if $\neq 0$.

Now, if we set $q = k = 0$ before the angular integration, the kernel vanishes for all $\cos \theta$, namely $K(0, 0; \cos \theta) = 0$. This is the standard argument that the effect of θ does not appear in the gap equation at extremely high density. However, if we first integrate over $\cos \theta$, and then take the limit $q, k \rightarrow 0$, the result is nonzero. This can be seen explicitly by carrying out the angular integral of K and by writing the result in terms of a variable $Y = (k+q)^2/(k^2+q^2) = 2$: becomes

$$\int_1^{Z_1} d\cos \theta K(q; k; \cos \theta) = \frac{Y-1}{2} \ln \frac{Y+1}{Y-1} - 1 : \quad (A3)$$

If we take the limit $Y \rightarrow 1$ in the right hand side, the first term disappears, but the second term survives and gives a gauge-dependent contribution. One can trace back the origin of this situation by introducing a small regulator to the collinear region of the integral $\cos \theta = 1$. Then, the integral above becomes

$$F(\theta; Y) = \int_1^{Z_1} d\cos \theta K(q; k; \cos \theta) = \frac{Y-1}{2} \ln \frac{Y+1}{Y-1} - \frac{Y-1}{Y+1} \frac{Y+1}{2} : \quad (A4)$$

The first term disappears irrespective of the order of $Y \rightarrow 1$ and $\theta \rightarrow 0$. However, the second term vanishes only when one takes $Y \rightarrow 1$ before $\theta \rightarrow 0$. Namely,

$$\lim_{Y \rightarrow 1} \lim_{\theta \rightarrow 0} F(\theta; Y) = 0; \quad (A5)$$

$$\lim_{\theta \rightarrow 0} \lim_{Y \rightarrow 1} F(\theta; Y) = : \quad (A6)$$

This non-commutability of the two limits arises from the fact that $F(\cdot; Y)$ does not approach to $F(0; Y)$ uniformly in the region $Y \rightarrow 1$.

Therefore, if we integrate over the angular variable $\cos \theta$ exactly, the gap equation for $\Delta_+(k)$ at high density has an extra gauge-dependent contribution from the quark-pole;

$$I(k) = \frac{g^2}{24^2} \int_0^{\infty} \frac{dq}{q} \frac{\Delta_+(q)}{E_+(q)^2 + \Delta_+(q)^2} \frac{q}{k} - 1 - \frac{(q - k)^2}{4qk} \ln \frac{(k + q)^2}{(k - q)^2} \quad : \quad (A7)$$

Compared with the leading magnetic contribution with the kernel of logarithmic singularity, the above contribution is considered to be a sub-leading effect.

APPENDIX B: PIPPARD LENGTH IN THE WEAK-COUPLING LIMIT

In this Appendix, we derive the Pippard length from the correlation function in the weak-coupling region. We use the two-point correlation function of quarks defined in Eq. (2.34)

$$\Delta_+(q) = \frac{p}{E_+(q)^2 + \Delta_+(q)^2}; \quad (B1)$$

Since $\Delta_+(q)$ is a function of $q > 0$ only, its Fourier transformation is given by

$$\begin{aligned} \Delta_+(r) &= \frac{N}{2^2} \int_0^{\infty} dq q^2 j_0(qr) \Delta_+(q); \\ &= \frac{N}{2^2 r} \int_0^{\infty} dq \sin(qr) \frac{q}{(q^2 + \Delta_+(q)^2)}; \end{aligned} \quad (B2)$$

where $j_0(x) = x^{-1} \sin x$ is the 0-th order spherical Bessel function.

In the weak-coupling limit, the integral is dominated at $q \rightarrow 0$. Then, by replacing $\Delta_+(q)$ and performing the q integration approximately, one finds

$$\begin{aligned} \Delta_+(r) &= \frac{N}{2^2 r} \int_0^{\infty} dq \sin(qr) \frac{q}{(q^2 + \Delta_+(0)^2)} \\ &= \frac{N}{2} \frac{\sin(r)}{r} \frac{\Delta_+(0)}{K_0(\Delta_+(0)r)}; \end{aligned} \quad (B3)$$

where K_0 is the 0-th modified Bessel function of the second kind. Using its asymptotic form

$$K_0(z) \sim \frac{1}{2z} e^{-z} \sum_{n=0}^{\infty} \frac{(n+1=2)}{(n+1=2)n!(2z)^n};$$

we obtain

$$\Delta_+(r) \sim \frac{1}{N} \frac{r}{2^3} \frac{\Delta_+(0)}{\Delta_+(0)^5} \frac{\sin(r)}{(r)^{3=2}} e^{-r/\Delta_+(0)}; \quad (B4)$$

where $\Delta_+(0)^{-1}$ is the Pippard length.

[1] J. C. Collins and M. J. Perry, *Phys. Rev. Lett.* **34**, 1353 (1975).

[2] D. Bailin and A. Love, *Phys. Rept.* **107**, 325 (1984).

[3] M. Iwasaki and T. Iwado, *Phys. Lett. B* **350**, 163 (1995); *Prog. Theor. Phys.* **94**, 1073 (1995).

[4] M. Alford, K. Rajagopal, and F. Wilczek, *Phys. Lett. B* **422**, 247 (1998).

[5] R. Rapp, T. Schafer, E. V. Shuryak, and M. Velkovsky, *Phys. Rev. Lett.* **81**, 53 (1998).

[6] For a recent review, see K. Rajagopal and F. Wilczek, "The Condensed Matter Physics of QCD", in "At the frontier of particle physics (handbook of QCD)", Volume 3, Chapter 35, edited by M. Shifman (World Scientific, 2001) [hep-ph/0011333].

[7] D. T. Son, *Phys. Rev. D* **59**, 094019 (1999).

[8] T. Schafer and F. Wilczek, *Phys. Rev. D* **60**, 114033 (1999).

[9] D. K. Hong, V. A. Miransky, I. A. Shovkovy and L. C. R. Wijewardhana, *Phys. Rev. D* **61**, 056001 (2000), Erratum -ibid. D **62** (2000) 059903.

[10] S. D. H. Hsu and M. Schwetz, *Nucl. Phys. B* **581**, 391 (2000).

[11] R. D. Pisarski and D. H. Rischke, *Phys. Rev. D* **61**, 074017 (2000).

[12] W. E. Brown, J. T. Liu, and H. C. Ren, *Phys. Rev. D* **61**, 114012 (2000); *ibid. D* **62**, 054013 (2000); *ibid. D* **62**, 054016 (2000).

[13] J. R. Schrieffer, "Theory of Superconductivity", (Benjamin, New York, 1964).

[14] R. Horie, "On Color Superconductivity in High Density Quark Matter", Master Thesis (Kyoto University, Feb. 1999),

[15] M. Matsuzaki, *Phys. Rev. D* **62**, 017501 (2000).

[16] M. Alford, K. Rajagopal, and F. Wilczek, *Nucl. Phys. B* **537**, 443 (1999).

[17] J. Berges and K. Rajagopal, *Nucl. Phys. B* **538**, 215 (1999).

[18] G. W. Carter and D. D. Iakonov, *Phys. Rev. D* **60** (1999) 016004.

[19] M. LeBellac, "Thermal Field Theory" (Cambridge University Press, 1996).

[20] K. Iida and G. Baym, *Phys. Rev. D* **63**, 074018 (2001).

[21] K. Rajagopal and E. Shuster, *Phys. Rev. D* **62**, 085007 (2000).

[22] K. Higashijima, *Phys. Rev. D* **29**, 1228 (1984); *Prog. Theor. Phys. Suppl.* **104**, 1 (1991).
V. A. Miransky, *Sov. J. Nucl. Phys.* **38**, 280 (1983).

[23] T. Kugo, "Basic Concepts in Dynamical Symmetry Breaking and Bound State Problems", lectures in 1991 Nagoya Spring School on Dynamical Symmetry Breaking (April 23-27, 1991, Nagoya, Japan) Ed. K. Yamawaki (World Scientific).
V. A. Miransky, "Dynamical Symmetry Breaking in Quantum Field Theories" (World Scientific, 1993).

[24] K.-I. Aoki, T. Kugo and M. M. Itchard, *Phys. Lett. B* **266**, 467 (1991). K.-I. Aoki, M. Bando, T. Kugo and M. M. Itchard, *Prog. Theor. Phys.* **84**, 683 (1990).

[25] A. L. Fetter and J. D. Walecka, "Quantum Theory of Many-Particle Systems" (McGraw-Hill, 1971).

[26] See e.g., P. Nozieres and S. Schmitt-Rink, *J. Low Temp. Phys.* **59**, 195 (1985).

[27] C. Manuel, *Phys. Rev. D* **62**, 114008 (2000).

[28] See e.g., D. J. Scalapino, in *Superconductivity*, edited by R. D. Parks (Dekker, New York, 1969).

[29] H. Abuki, T. Hatsuda, and K. Itakura, work in progress.

[30] H. Abuki, "Color Superconductivity in Quark Matter at High Density" Master Thesis (Kyoto University, Feb. 2000)

[31] P. Ring and P. Schuck, "Nuclear Many-Body Problem" (Springer, New York, 1980).